NEUROSCIENCE

Selective and coherent activity increases due to stimulation indicate functional distinctions between episodic memory networks

Sungshin Kim[1,2,3]*, Aneesha S. Nilakantan[1]*, Molly S. Hermiller[1], Robert T. Palumbo[1], Stephen VanHaerents[1], Joel L. Voss[1†]

Posterior-medial and anterior-temporal cortical networks interact with the hippocampus and are thought to distinctly support episodic memory. We causally tested this putative distinction by determining whether targeted noninvasive stimulation could selectively affect neural signals of memory formation within the posterior-medial network. Stimulation enhanced the posterior-medial network's evoked response to stimuli during memory formation, and this activity increase was coherent throughout the network. In contrast, there was no increase in anterior-temporal network activity due to stimulation. In addition, control stimulation of an out-of-network prefrontal cortex location in a separate group of subjects did not influence memory-related activity in either network. The posterior-medial network is therefore a functional unit for memory processing that is distinct from the anterior-temporal network. These findings suggest that targeted stimulation can lead to network-specific increases in excitability during memory formation and hold promise for efforts to fine-tune network involvement in episodic memory via brain stimulation.

INTRODUCTION

The hippocampus is necessary for episodic memory (*1*), and recent theories emphasize its interaction with nearby medial temporal cortex and widely distributed neocortical regions (*2*–*5*). Following evidence for functional distinction of parahippocampal and perirhinal cortex (*5*–*10*), distinct posterior versus anterior networks have been hypothesized (*11*–*14*). Distinctions have been proposed between a posterior-medial (PM) network, which includes retrosplenial, posterior-cingulate, precuneus, parahippocampal, and lateral-parietal cortex, and an anterior-temporal (AT) network, which includes ventral anterior temporal, lateral orbitofrontal, prefrontal, and perirhinal cortex (*5*, *15*). PM and AT network regions respond as distinct functional units during memory processing, with regions of each network showing similar activity profiles and specialization for different categories of memory (*15*–*18*). However, measures of neural activity [including indirect indicators such as functional magnetic resonance imaging (fMRI)] are correlative and therefore cannot substantiate these functional distinctions alone. Although experiments involving individuals with brain lesions are the current standard for causal tests in humans, focal lesions can negatively affect broad network organization, often disrupting multiple networks and cognitive abilities (*19*–*22*). Thus, the distinction between PM and AT activity profiles observed during memory processing has not been causally tested. We sought to provide such a test by using noninvasive brain stimulation to selectively modulate memory processing within one network relative to the other.

We have previously demonstrated that network-targeted transcranial magnetic stimulation (TMS) can increase interregional correlations of fMRI activity among regions of the hippocampal-cortical network measured during the resting state (*23*). However, it is unclear how these changes in resting-state activity relate to memory improvements that also occurred because of stimulation (*23*, *24*). Specific changes in memory processing by networks have never been demonstrated via stimulation before. Selective modulation of memory-related neural activity would show that these networks can be manipulated independently and therefore operate as discrete units. Furthermore, the nature of activity changes during memory processing could implicate specific mechanisms by which noninvasive stimulation alters hippocampal-cortical network function. For instance, increases in stimulus-evoked activity would implicate increased neural excitability due to stimulation, similar to the widespread neural response facilitation observed in rodents following induction of hippocampal long-term potentiation (LTP) (*25*).

The present experiments therefore aimed to test whether targeted noninvasive stimulation selectively alters stimulus-evoked activity of the PM versus AT networks during memory formation. We measured fMRI activity while human subjects studied item-context associations using memory tests with two different formats. To determine whether the PM network responded to stimulation as a functional unit, we assessed the coherence of activity changes caused by stimulation among the regions comprising the network. We assessed effects of stimulation on fMRI activity during memory formation relative to low-intensity sham control stimulation. A separate control experiment in an independent group of subjects used the same stimulation and testing parameters as in the main experiment, but with stimulation delivered to the dorsolateral prefrontal cortex, which is distinct from PM-AT networks. We defined PM-AT network regions of interest for fMRI analyses a priori, and we also used whole-brain voxel-wise analyses to interrogate changes in the activity that may have occurred, distinct from these PM-AT regions of interest. These experiments thereby tested the putative functional

[1]Department of Medical Social Sciences, Ken and Ruth Davee Department of Neurology, Department of Psychiatry and Behavioral Sciences, and Interdepartmental Neuroscience Program, Feinberg School of Medicine, Northwestern University, Chicago, IL 60611, USA. [2]Center for Neuroscience Imaging Research, Institute for Basic Science, Suwon, Republic of Korea. [3]Sungkyunkwan University, Suwon, Republic of Korea.
*These authors contributed equally to this work.
†Corresponding author. Email: joel-voss@northwestern.edu

distinction between PM and AT networks by measuring changes in the coherence of memory-related activity due to PM-targeted versus control stimulation.

RESULTS

For the primary experiment in which the PM network was targeted via stimulation delivered to the lateral parietal cortex, 16 subjects completed a sham-controlled, counterbalanced paradigm. As in our previous experiments (*23*, *24*), stimulation involved five consecutive daily sessions of 20-Hz repetitive TMS. Stimulation was delivered to subject-specific parietal cortex locations defined on the basis of high baseline fMRI connectivity with the hippocampus (Fig. 1A). We selected this area of the parietal cortex because it demonstrates robust fMRI connectivity with the hippocampus and has direct projections to retrosplenial and parahippocampal cortex, which also provide input to the hippocampus (*26*, *27*). At each assessment (Pre-Stim, Pre-Sham, Post-Stim, and Post-Sham; Fig. 1B), we collected fMRI while participants studied stimuli in contextual memory tasks, which we administered in a counterbalanced order across participants (Fig. 1C). Primary analyses examined the activity evoked by stimuli during the study phase that subjects endorsed correctly (remembered) during the subsequent test, thereby providing a neural signal of episodic memory formation (*28*). We averaged the activity within PM and AT network regions of interest defined by previous studies (Fig. 2A) (*18*, *29*).

Activity evoked by later-remembered stimuli was negative for Baseline (combination of Pre-Stim and Pre-Sham) and also following sham stimulation (Post-Sham) for both the PM and AT networks (tables S1 and S2). Negative-going fMRI activity deflections are typical for these networks during memory tasks (*3*, *30*). To identify the effects of parietal stimulation on activity relative to sham, we compared the activity during the Post-Stim assessment versus Post-Sham assessment, computed separately for the contextual and spatial memory tasks and for the PM and AT networks (Fig. 2B). There was a main effect of network ($F_{1,15} = 11.77$, $P = 0.0037$, $\eta_p^2 = 0.44$) but no interaction of network by memory task ($F_{1,15} = 0.37$, $P = 0.55$). We identified the same pattern when we also considered Baseline activity, with a significant main effect of stimulation condition (Baseline, Post-Stim, and Post-Sham: $F_{2,30} = 4.87$, $P = 0.015$, $\eta_p^2 = 0.24$) and a significant interaction of network and stimulation condition ($F_{2,30} = 7.72$, $P = 0.0020$, $\eta_p^2 = 0.34$) but no significant interaction of stimulation by memory task ($F_{2,30} = 0.42$, $P = 0.66$). Thus, parietal stimulation differentially affected activity of the PM versus AT networks but without variation by memory test format. We therefore combined estimates of fMRI activity across memory test formats for all subsequent analyses.

Parietal stimulation increased activity relative to sham (Post-Stim versus Post-Sham) for all PM network regions collapsed together ($T_{15} = 4.08$, $P < 0.001$, Cohen's $d = 1.02$) but had no effect on AT network regions collapsed together ($T_{15} = 0.83$, $P = 0.42$) (Fig. 2B). The effect of stimulation on activity was significantly greater for the PM network than the AT network ($T_{15} = 3.43$, $P = 0.0037$, Cohen's $d = 0.86$). This demonstrates network-selective effects of stimulation on fMRI signals of memory formation. Notably, relative activity increases of hippocampal network regions are commonly associated with better memory formation (*28*, *31*), and therefore, the stimulation effects are consistent with improved stimulus-evoked memory processing by the PM network.

To evaluate the network-wide consistency of the effects of stimulation on fMRI activity, we analyzed the effects of stimulation separately for all regions comprising the PM and AT networks. The

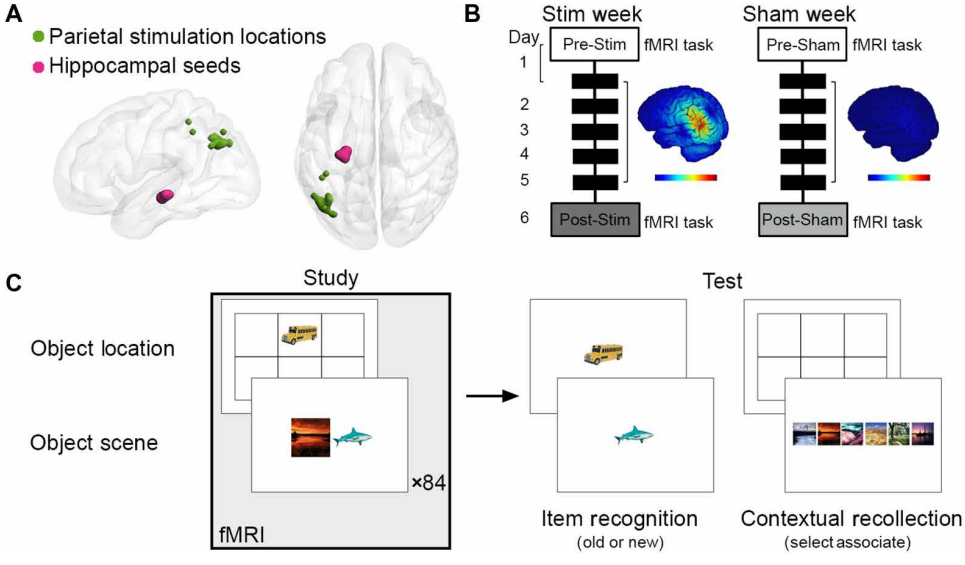

Fig. 1. Experiment design overview. (**A**) We selected subject-specific left parietal stimulation locations on the basis of seed-based resting-state fMRI connectivity with anatomically defined hippocampal locations. Circles indicate these locations for each participant. (**B**) Before and ~24 hours after five consecutive daily stimulation sessions, participants completed an fMRI memory task. We administered stimulation and sham conditions within subjects in a counterbalanced order. Representative electrical fields (e-fields) for one subject demonstrate stimulation and sham intensities, with red indicating peak intensity (color bar range, 1 to 210 V/m). (**C**) In separate blocks, participants studied trial-unique objects paired with either scene or location contexts during fMRI scanning. After a delay, we assessed object recognition memory and contextual recollection memory. Responses were used to identify trials during study that were later correct, thereby providing fMRI signals of successful memory formation. We used different stimuli for each fMRI task assessment.

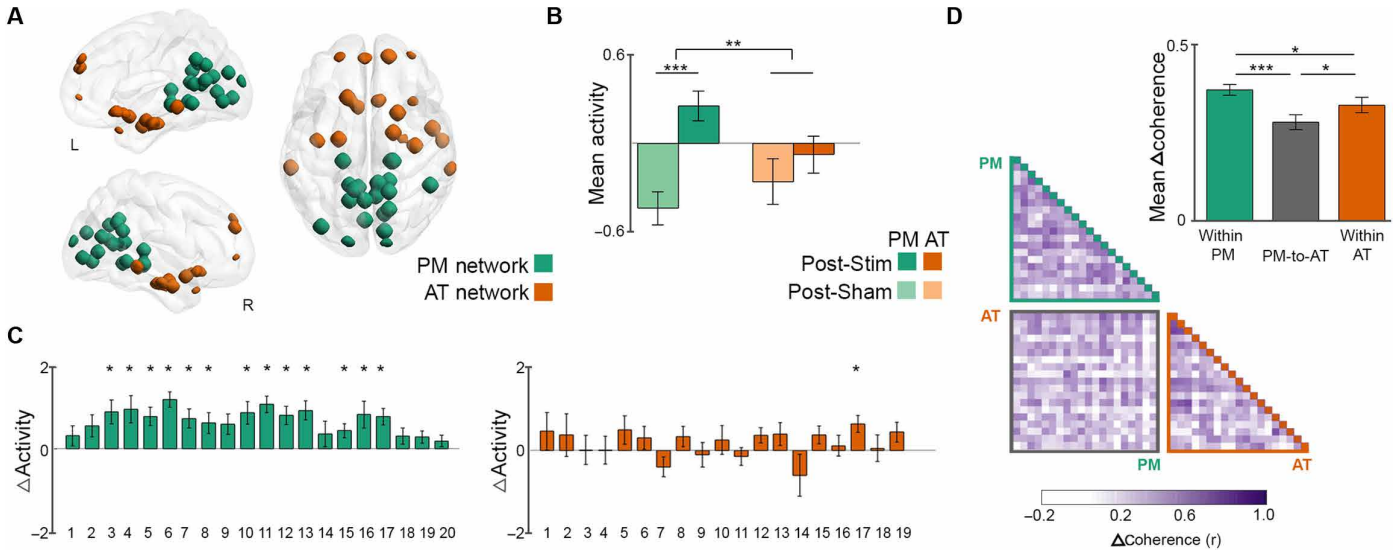

Fig. 2. Stimulation coherently increased PM network fMRI activity. (**A**) We selected PM and AT network regions of interest a priori (*18*, *29*). L, left; R, right. (**B**) Mean fMRI activity evoked by stimuli during memory formation averaged for the PM and AT networks for the Post-Stim and Post-Sham conditions, demonstrating selective increases in PM network activity due to stimulation (Post-Stim versus Post-Sham). (**C**) Mean fMRI activity changes due to stimulation (Post-Stim minus Post-Sham) averaged for each region within the PM and AT networks demonstrate consistent increases for the PM network but not for the AT network. (**D**) Coherence of activity changes due to stimulation is shown via a correlation graph, with coloration indicating between-region correlations of activity changes across subjects. We quantified the coherence as the mean correlation for each network and between networks, as indicated via bar graphs, demonstrating network-specific coherence of changes that were greatest for the PM network. Error bars indicate SEM. **P* < 0.05, ***P* < 0.01, and ****P* < 0.001.

effects of stimulation (Post-Stim versus Post-Sham) were positive in all individual PM network regions and significant (at $P < 0.05$ uncorrected) for 13 of 20 regions but for only 1 of 19 regions of the AT network (Fig. 2C and tables S1 and S2). Stimulation thus increased fMRI signals of memory formation throughout the PM network.

We next tested whether parietal stimulation coherently changed fMRI activity within each network. We calculated changes in activity due to stimulation (Post-Stim versus Post-Sham) for each region of the PM and AT networks and measured the coherence of activity changes due to stimulation as the mean of the region-to-region correlations in activity across subjects (see Materials and Methods). The effects of stimulation on the activity change coherence were significantly greater for the PM network than for the AT network ($T_{37} = 2.22$, $P = 0.033$, Cohen's $d = 0.71$) and significantly greater within the PM network than between the PM and AT networks ($T_{19} = 5.91$, $P < 0.0001$, Cohen's $d = 1.32$) (Fig. 2D). The coherence of activity change was also significantly greater within the AT network than between the PM and AT networks ($T_{18} = 2.78$, $P = 0.012$, Cohen's $d = 0.64$). These findings indicate that the regions comprising the PM and AT networks responded to stimulation as coherent and distinct units, with greater coherence of activity changes within each network relative to between networks and with the greatest coherence of activity changes occurring for the PM network.

Although the aforementioned analyses using network regions of interest are advantageous in providing strong tests of a priori PM-AT regions and controlling for the possibility of false positives, they do not test the possibility that stimulation could have affected any out-of-network fMRI activity. To address this, we conducted whole-brain, voxel-wise analyses using a stringent threshold. Regions with increased evoked activity (Post-Stim versus Post-Sham) included inferior temporal, medial parietal-occipital, and parahippocampal cortical areas (Fig. 3A and table S3), with no regions showing decreased activity. Notably, the results from this voxel-wise analysis overlap substantially with the PM network regions of interest, with no evidence for the effects of stimulation on activity outside of areas typically classified as the PM network.

We tested the duration of stimulation effects on the PM network via follow-up assessment 1 week following the Post-Stim and Post-Sham sessions. fMRI activity was at approximately baseline levels at follow-up, with no significant PM network activity difference relative to the Post-Sham Follow-up session ($T_{15} = 0.29$, $P = 0.78$). Follow-up PM network activity in the stimulation condition was significantly reduced relative to the Post-Stim assessment ($T_{15} = 3.19$, $P = 0.0061$), indicating a significant decline to baseline levels. The AT network had no activity differences for the stimulation and sham conditions at follow-up assessment ($P > 0.1$), as was the case for the 24-hour assessments. We thus observed increased PM network activity ~24 hours following stimulation, but it had returned to approximately baseline by ~1 week following stimulation.

As was the case in our previous studies in cognitively normal young adults (*23*, *24*), stimulation modestly improved contextual recollection, which was assessed separately from item recognition (Fig. 1C). Of these two memory expressions, only contextual recollection is thought to depend heavily on the hippocampus and PM network (*15*). On the basis of our previous demonstrations of improved recollection due to stimulation (*23*, *24*), we hypothesized that stimulation would improve contextual recollection accuracy, which we therefore tested directionally. Stimulation did not improve item recognition accuracy (Post-Stim versus Post-Sham: $T_{15} = 0.46$, $P = 0.68$; Fig. 3B). Also as hypothesized, contextual recollection accuracy improved because of stimulation (Post-Stim versus Post-Sham: $T_{15} = 2.02$, $P = 0.031$, Cohen's $d = 0.51$; Fig. 3, C and D). These findings indicate that increases in PM network activity due to

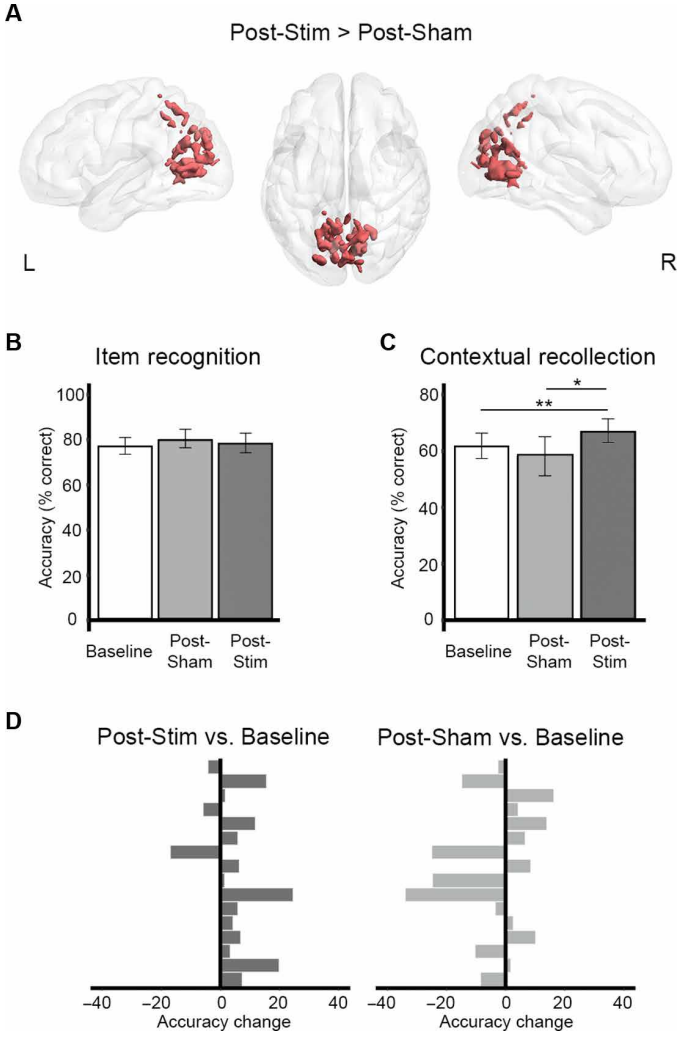

Fig. 3. Effects of stimulation on voxel-level activity and memory performance. (**A**) Whole-brain, voxel-wise analyses show regions of significant activity change due to stimulation (Post-Stim minus Post-Sham) unconstrained by the PM-AT network regions of interest. Coloration indicates voxels meeting the significance threshold (see Materials and Methods), which all showed greater activity Post-Stim versus Post-Sham in the PM network regions (table S3). (**B**) Mean item recognition did not change because of stimulation. (**C**) Mean contextual recollection increased because of stimulation, relative to Baseline and relative to sham. (**D**) Each bar represents a single subject change in contextual recollection accuracy Post-Stim relative to Baseline and Post-Sham relative to Baseline, showing that stimulation consistently improved contextual recollection, whereas increases occurred in only ~50% of subjects due to sham. Error bars indicate SEM. *P < 0.05 and **P < 0.025 (one-tailed).

stimulation occurred concomitantly with modest improvements in memory, specifically for the contextual recollection component thought to rely on this network.

To provide an out-of-network active control stimulation condition, a separate group of 16 subjects completed the same sham-controlled counterbalanced experiment but with stimulation of left dorsolateral prefrontal cortex (Fig. 4A). We selected this area of dorsolateral prefrontal cortex as an active control because it is involved in episodic memory (*32*) but does not have robust fMRI connectivity with the hippocampus at rest or direct anatomical projections to the medial temporal lobe (*12*). Thus, to the extent that stimulation applied to any location demonstrating memory-related fMRI activity affects PM network activity, we would have expected similar results in the active control condition as in the main parietal stimulation condition. However, if influencing PM network activity requires stimulation of locations having high connectivity with this network, then we would have expected no PM network effects of stimulation relative to sham in the active control condition.

Active control stimulation of the prefrontal cortex did not cause significant changes in PM or AT activity (Fig. 4B). To determine whether parietal stimulation effects on PM network activity (Figs. 2 and 3) were significantly greater than the effects caused by prefrontal control stimulation, we made between-group pairwise comparisons for the Baseline, Post-Sham, and Post-Stim assessments using activity averaged separately for the PM and AT networks. The only significant between-group difference was greater activity Post-Stim for parietal stimulation relative to prefrontal control stimulation for the PM network (T_{30} = 3.66, P < 0.001, Cohen's d = 1.29; all other comparisons, P > 0.2). Thus, the primary effect that resulted from parietal stimulation (increased PM activity Post-Stim) was therefore a selective result of parietal stimulation relative to prefrontal control stimulation.

Whole-brain voxel-wise analyses for the prefrontal control stimulation condition (Post-Stim versus Post-Sham) identified no significant clusters of fMRI activity changes due to stimulation in the PM-AT network regions. Prefrontal control stimulation caused significant reduction of activity in dorsolateral prefrontal cortex contralateral to the stimulation location, indicating that prefrontal stimulation led to changes in neural signals of memory formation in an area distinct from the PM-AT networks (table S5). Between-group analysis indicated that activity increases in subjects receiving parietal stimulation were significantly greater than activity changes in subjects receiving prefrontal control stimulation, selectively within regions typical of the PM network (Fig. 4C and table S5). We likewise hypothesized that active control stimulation of prefrontal cortex would not significantly improve contextual recollection accuracy, and it did not (Post-Stim versus Post-Sham: T_{15} = 0.432, P = 0.664), nor did it improve item recognition accuracy (T_{15} = 1.37, P = 0.90). Between-group comparisons testing the hypothesis that parietal stimulation would produce greater contextual recollection improvement than prefrontal control stimulation indicated that the improvement due to stimulation (Post-Stim versus Post-Sham) was greater for the subjects receiving parietal stimulation (T_{30} = 2.00, P = 0.027, Cohen's d = 0.71). These between-group differences confirm that enhanced activity of the PM network and contextual recollection improvements were specific for parietal stimulation targeting the PM network, relative to prefrontal control stimulation.

DISCUSSION

Targeted stimulation increased fMRI activity evoked by subsequently remembered stimuli during memory formation throughout the PM network. The memory-related changes in activity were selective, as there were no significant effects within the AT network (Fig. 2B). Furthermore, activity increases due to stimulation were coherent throughout the PM network (Fig. 2, C and D) and were concomitant with modest gains in the accuracy of contextual recollection (Fig. 3, C and D), which is thought to rely on the PM network (*5*, *15*). Active control stimulation of the dorsolateral prefrontal

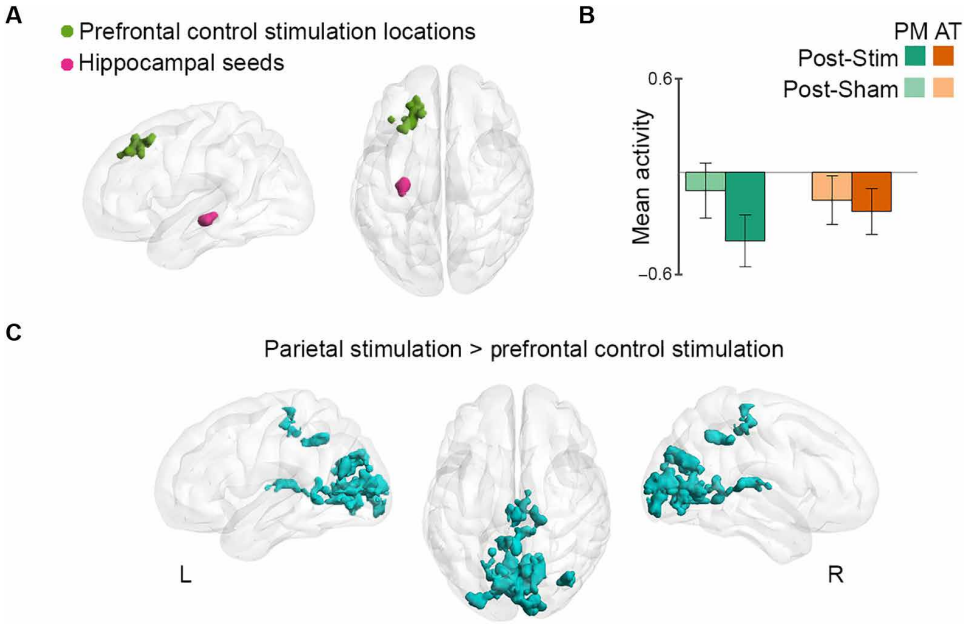

Fig. 4. Prefrontal control stimulation did not affect the PM network. (**A**) Prefrontal locations used for control stimulation are shown following the format of Fig. 1A. (**B**) Mean fMRI activity evoked by stimuli during memory formation averaged for the PM and AT networks for the Post-Stim and Post-Sham conditions, indicating no significant effects of stimulation. Effects of stimulation on the PM network were significantly greater for subjects receiving parietal stimulation than those receiving prefrontal control stimulation (not shown, see text). (**C**) Whole-brain, voxel-wise analyses indicated that there were no significant effects of stimulation on activity (Post-Stim versus Post-Sham) for the prefrontal control group in PM-AT network areas, but there were significant decreases in right dorsolateral prefrontal cortex activity (not shown, see text and table S4). Coloration indicates areas where there were significant between-group differences, reflecting greater activity increases due to stimulation (Post-Stim versus Post-Sham) for the parietal stimulation group relative to the prefrontal control stimulation group. Notably, these areas were located within the PM network, confirming that PM network activity increased selectively for parietal stimulation relative to prefrontal control stimulation (table S5).

cortex, a region involved in memory processing but distinct from the PM-AT networks, did not influence PM or AT network activity in a separate control group. Between-group comparisons confirmed that PM activity increases due to parietal stimulation were significantly greater than any changes that occurred because of prefrontal control stimulation (Fig. 4). Thus, parietal stimulation targeting the PM network was selective in increasing activity coherently only within the PM network. The PM network thus changed in its stimulus-related processing as a functional unit distinct from the AT network due to targeted stimulation. These findings support the functional significance of cohesive, network-specific activity profiles identified for the hippocampal-cortical network using fMRI, thereby causally validating the functional distinction of PM from the AT networks.

The PM network regions with increased activity due to targeted stimulation were distant from the location of lateral parietal cortex that was stimulated, including medial and lateral occipital-parietal regions and medial temporal lobe. Notably, the analyses of evoked activity used here provide location-specific metrics of functional changes due to stimulation. In contrast, a previous demonstration of alterations in hippocampal fMRI connectivity due to this stimulation regimen (*23*) was not location-specific, in that fMRI connectivity reflects changes in correlated activity between two or more regions and therefore cannot be attributed to functional changes occurring at any one location. These findings indicate that brain stimulation can have downstream effects on the functional engagement of specific brain regions in cognitive processing, distinct from any potential local effects.

Stimulus-evoked activity increases that resulted from stimulation suggest heightened excitability throughout the PM network. That is, given the same category of visual stimulus, PM network regions exhibited greater evoked responses after stimulation relative to before stimulation. This has not been previously demonstrated in humans, although there is considerable evidence that greater neural excitability is associated with better memory ability in animal models (*33*). Mechanisms for network-level excitability, as implicated by the current findings, are unknown. Greater stimulus-evoked responses could either cause or result from facilitated neural communication throughout the network (*34*). Experiments in rodents indicate that induction of long-term potentiation (LTP) within the hippocampus results in increased connectivity throughout the distributed hippocampal-cortical network, as measured by stimulation-evoked responses (*25*, *35*). Thus, increased synaptic efficacy due to LTP can cause increased network-level functional coupling. Notably, we previously demonstrated increased resting-state fMRI connectivity of the PM network following stimulation (*23*). It is possible that stimulation increases functional coupling of PM regions and the hippocampus via an LTP-like mechanism, which thereby synchronizes memory processing throughout the network, yielding enhanced stimulus-evoked activity and memory performance. However, systematic testing of the many possible neuronal mechanisms for increased functional coupling and stimulus-evoked activity due to stimulation will require the development of relevant animal models.

Increased PM network evoked activity due to stimulation was concomitant with improved contextual recollection, but no change occurred in object recognition. This is notable given that the PM

network and hippocampus have been implicated particularly in contextual recollection aspects of memory (*15*, *36*) and is consistent with our previous findings of recollection-specific improvement using this targeted stimulation method (*23*, *24*). Many previous findings have indicated that relative activity increases are neural signals of successful memory formation (*28*, *31*). However, this conclusion is based primarily on natural variation in activity levels across stimuli, which could result from a variety of factors. The current findings causally support the link between relative activity increase and memory formation by showing that both respond concurrently to stimulation. Note that the effects of stimulation on contextual recollection were statistically modest, with an effect size typically classified as "medium," whereas the effects of stimulation on fMRI activity were highly robust, with an effect size classified as "large." This indicates that many factors other than PM network activity during memory formation likely govern subsequent memory performance. However, note that subjects in the current experiment were cognitively normal young adults, with PM network function that was likely near-optimal for each individual at baseline. The effects of stimulation on PM networks with suboptimal function are unknown, with some evidence from rodent models indicating that manipulations affecting neural excitability have greater benefits for memory-impaired versus memory-intact subjects (*33*).

In summary, targeted stimulation selectively and coherently enhanced activity evoked by stimuli during memory formation for the PM network and improved contextual recollection memory. These findings provide a novel demonstration that networks defined primarily by fMRI are units of organization that can be directly and coherently manipulated. The results validate putative PM versus AT network subdivisions, support the functional significance of activity distributed across networks, and corroborate the role of relative activity increases in memory formation. Although additional evidence is needed to evaluate whether optimized stimulation regimens could produce more robust and persistent changes, the relatively long-lasting (~24 hours) and network-specific stimulation effects on task-relevant processing hold promise for the development of targeted treatments for disorders related to hippocampal-cortical network dysfunction (*3*, *37*). As demonstrated by the current experiment, it is likely that these treatments will require the ability to manipulate excitability throughout the discrete yet distributed networks that support cognition (*38*).

MATERIALS AND METHODS

Participants

Sixteen adults participated in the main experiment using parietal stimulation to target the PM network (11 females; mean age, 26.06 years; range, 18 to 34 years), and a separate 16 adults participated in the dorsolateral prefrontal active-control stimulation experiment (10 females; mean age, 25.4 years; range, 18 to 34 years). Data from an additional subject were collected but discarded from analyses because of excessive in-scanner movement and poor overall memory performance. All conditions of interest were fully counterbalanced in the final sample contributing data to analyses. All participants had normal or correct-to-normal vision and did not report any history of neurological or psychiatric disorders or current drug use. Participants were eligible for MRI and TMS procedures according to standard MRI and TMS safety-screening questionnaires (*39*). Eligibility contraindications were evaluated by a neurologist (S.V.). Participants provided written informed consent and were monetarily compensated. The Institutional Review Board at Northwestern University approved all procedures.

Experimental design

Participants completed a 2-week experiment involving 1 week of full-intensity stimulation and 1 week of sham stimulation. The order of these 2 weeks was counterbalanced, and the first day of each week was separated by a delay of at least 4 weeks (mean interval, 10.10 weeks; range, 4.71 to 29.86 weeks for the parietal stimulation condition; mean interval, 13.17 weeks; range, 6.00 to 37.14 weeks for the prefrontal control stimulation condition). About 2 hours before receiving stimulation on the first day of each week and ~24 hours after five consecutive daily stimulation sessions (mean delay, 22.70 hours; SD, 2.08 hours from the final stimulation session), participants completed one of six versions of the fMRI memory task (see below). After each week, participants also completed a 1-week follow-up, including a new version of the fMRI memory task on each day. Some assessments also included additional MRI scans and a battery of out-of-scanner cognitive tests; these ancillary data are not described in this study. Post-sham data in the parietal stimulation group were not available for one subject due to technical malfunction, and so they were replaced by 1-week follow-up data.

Identification of stimulation locations

For targeted stimulation, individualized left lateral parietal stimulation locations were determined on the basis of high resting-state fMRI connectivity with a left hippocampal seed using a procedure previously described (*23*). Resting-state scanning was performed on the first visit before any task-based fMRI using a whole-brain blood oxygen level–dependent (BOLD) echo-planar imaging sequence [T_R = 555 ms; T_E = 22 ms; field of view (FOV), 208 × 196 mm; flip angle, 47°; voxel resolution, 2.0 × 2.0 × 2.0 mm; 550 volumes; multiband acceleration factor, 8 (*40*)]. During the ~5-min resting-state scan, participants were instructed to lie still, fixate on a cross at the center of the screen, and rest with their eyes open. Preprocessing included slice-time correction, functional-structural co-registration, stereotactic transformation using TT_N27 template, spatial smoothing of 4-mm full width at half maximum Gaussian kernel, despiking, and linear detrending. A hippocampal volume of interest was identified for each participant by identifying a voxel in the body of the left hippocampus closest to MNI [−29, −25, −13] for which fMRI connectivity was maximal to contralateral hippocampus (mean distance, 3.06 mm; range, 0.00 to 10.05 mm for parietal stimulation group; mean distance, 2.88 mm; range, 1.00 to 6.71 mm for the prefrontal stimulation control group). This location was used for seed-based connectivity analysis (InstaCorr) using a seed radius of 2 mm and including the motion time series as a regressor of no interest and a bandpass filtering from 0.01 to 0.1 Hz.

For the parietal stimulation group, the stimulation location was selected as the peak connectivity cluster within the left lateral parietal cortex, within an anatomical mask of angular gyrus and superior and inferior parietal lobule close to MNI [−47, −68, 36] (mean distance, 7.42 mm; range, 0.0 to 14.46 mm from this coordinate; Fig. 1A). For the prefrontal control stimulation group, the stimulation location was selected as the peak connectivity cluster within a functional mask of left dorsolateral prefrontal cortex (Fig. 4A). This mask was generated by Neurosynth (on 28 April 2016) as meta-analytic coactivation with the left hippocampus [MNI −29, −25, −13]. Notably, the dorsolateral prefrontal region had minimal group-level

fMRI resting-state connectivity with the hippocampus, despite functional coactivation, indicating a relationship to the hippocampus related to memory, but weak functional connectivity. The stimulation target was transformed for each participant to original space for anatomically guided stimulation. The same stimulation location was used for each subject for both stimulation and sham weeks.

Transcranial magnetic stimulation

The MagPro X100 system with a MagPro Cool-B65 liquid-cooled butterfly coil was used (MagVenture A/S). A frameless stereotactic system (Localite GmbH) used individual MRIs for anatomical targeting of stimulation and recording coil locations relative to the brain for each TMS pulse. Resting motor threshold (MT) was determined visually on the basis of the minimum stimulator output required to generate a contraction of the abductor pollicis brevis for 5 of 10 consecutive single pulses. Repetitive TMS was planned at 100% MT for each day of the stimulation week and at 10% MT for each day of the sham week, although these values were lowered because of discomfort for five subjects in the parietal stimulation group (to 95, 90, 82, 80, and 72% MT) and for three subjects in the prefrontal control group (to 89, 83, and 74% MT). The final mean stimulator output intensity for stimulation was 52.37 (SD, 8.2) for the parietal stimulation group and 50.1 (SD, 4.87) for the prefrontal control group, and for sham was 5.63 (SD, 0.89) for the parietal stimulation group and 5.18 (SD, 0.65) for the prefrontal control group. Each daily TMS session consisted of 40 consecutive trains of 20-Hz pulses for 2 s, followed by 28 s of no stimulation (1600 pulses per session, a total of 20 min).

The TMS coil location and the stimulator current rate of change (*dI/dt*) were recorded digitally. For visualization, TMS-induced e-fields were estimated using SimNIBS 2.0 (*41*). Tetrahedral head meshes segmented by tissue class (white matter, gray matter, cerebrospinal fluid, skull, and skin) were created for each subject from the T1-weighted magnetic resonance images. The coordinates of the coil position, recorded during each session, were transformed (Localite GmbH) to the individual mesh space. These coordinates, along with the recorded *dI/dt* from the stimulator, were used in a realistic finite element model. The head meshes were converted to volumetric maps in each subject's native space and then spatially normalized to standardized space using the same approach as was used for fMRI analysis.

Task-based fMRI

MRI data were acquired using a Siemens 3T TIM Prisma whole-body scanner with a 64-channel head/neck coil. Whole-brain functional images were acquired during the tasks, with a 2000-ms repetition time, a 20-ms echo time, a 210 × 203 mm FOV, an 80° flip angle, 1.7 × 1.7 × 1.7 mm isotropic voxels, and a multiband factor of 2. The duration of each scan at study varied slightly on the basis of interstimulus interval randomization, varying from 115 to 132 volumes for the object-scene task and from 117 to 133 volumes for the object-location task. There was no significant difference in the duration between tasks or sessions (all $P > 0.3$). fMRI data were acquired during the study and test portions of each test, but only study-phase data were analyzed here. A structural image was also acquired to provide anatomical localization (MP RAGE T1-weighted scans; with T_R = 2170 ms, T_E = 1.69 ms, 256-mm FOV, 7° flip angle, and 1.0 × 1.0 × 1.0 mm voxel resolution over 176 sagittal slices).

The memory task completed at each assessment (Pre-Stim, Post-Stim, Pre-Sham, Post-Sham, Stim Follow-up, and Sham Follow-up) involved study-test blocks and used two stimulus formats. For object-scene blocks, participants studied 42 trial-unique objects [3 × 3 degrees of visual angle (*42*)], each paired with one of six scenes [3 × 3 degrees of visual angle (*43*)], and then, memory was tested after a 2-min delay. For object-location blocks, participants studied 42 trial-unique objects, each shown at one of six locations on a grid (6 × 9 degrees of visual angle), and then, memory was tested after a 2-min delay. During study, each paired object-context stimulus was presented for 1.5 s, followed by an interstimulus interval (mean interval, 4 s; range, 2 to 6 s). For memory testing, the first three and last three stimuli presented during study were not tested to reduce primacy/recency effects. For each block, there were 72 test trials, half including old (studied) objects and half including new (unstudied) objects, each presented at the center of the screen for 2 s, followed by an interstimulus interval (mean interval, 4 s; range, 2 to 6 s). Participants first categorized object as "old" or "new" and simultaneously rated confidence as "certain" or "uncertain" using four response options, providing a measure of item recognition memory. Participants had 3 s to make each response. All old/studied objects were then tested for contextual recollection memory, whereby participants selected the scene or the location associated with the object during the study phase. Participants had up to 5 s to respond. After the response period, there was a random interstimulus interval (mean interval, 4 s; range, 2 to 6 s) before the next trial. The parietal stimulation and prefrontal control stimulation groups were matched such that one subject in each group received the identical version of the experiment (stimuli assignments to conditions, order of conditions, etc.).

Participants viewed the task on an MRI-compatible liquid crystal display monitor viewed via a mirror mounted to the head coil. Participants used an MRI-compatible optical mouse to register all responses. The order of object-scene and object-location study-test blocks was counterbalanced across experimental conditions and sessions. Distinct sets of trial-unique objects and session-unique scene images were used for each assessment, with assignment counterbalanced across experimental conditions and sessions.

Stimulus-evoked activity analysis

fMRI data were processed using AFNI software version 4.56 (*44*), and findings were visualized using BrainNet Viewer (*45*). Preprocessing included the same steps used by resting-state fMRI for target identification (described above). Trials at study were back-sorted according to responses during the delayed test phase such that they could be categorized as later-remembered (hits) and later-forgotten (misses), irrespective of confidence.

Activity associated with later-remembered trials was calculated during the study phase for both tasks. The BOLD hemodynamic response was modeled as seven tent functions from 0 to 12 s after each stimulus onset with peaks every 2 s, aligned to the T_R. General linear modeling with hemodynamic response deconvolution (3dDeconvolve) included stimulus onsets of later-remembered trials, stimulus onsets of all other trials (later-forgotten response, later-missed response, and primacy and recency buffer trials), and six estimates of motion, translations, and rotations (pitch, roll, and yaw) in three dimensions. Activity was calculated as the sum of the seven tent-function β coefficients separately for each task or aggregated across tasks. Main analyses included comparisons of Post-Stim and Post-Sham activity estimates (3dttest++), as well as comparisons versus Baseline, which was calculated using data concatenated

across the Pre-Stim and Pre-Sham assessments separately for each test format. There were no significant differences in trial counts for any conditions of interest for either the parietal stimulation or prefrontal control stimulation groups ($P > 0.1$).

The main PM-AT analysis (Fig. 2A) used a priori network regions identified in previous studies based on fMRI connectivity with parahippocampal and perirhinal cortex, respectively (*18*, *29*). Regions of interest were 6-mm-radius spheres centered on peak coordinates of each network location (described in tables S1 and S2). Only voxels that overlapped with a group-level mask generated on the basis of the intersection of all individual-subject masks (3dAutomask) were included. The left frontopolar cortex region was excluded from the AT network because some subjects had signal dropout in this region. Four voxels overlapped between the right medial posterior occipital cortex and the right retrosplenial cortex, and these voxels were reassigned to the region of interest with the closest center coordinate. Mean activity for later-remembered trials was calculated for each region for object-scene and object-location tasks, as well as aggregated across tasks. Mean activity was averaged across all regions within each network for some analyses. To measure the coherence of activity changes within networks (Fig. 2, C and D), we first calculated all pairwise region-to-region correlations of activity change across subjects (Post-Stim versus Post-Sham), yielding a 39-by-39 correlation matrix (20 PM regions and 19 AT regions). Then, we calculated the mean correlation values within each network and between the networks.

The whole-brain, voxel-wise analysis (Fig. 3A) used group-level *t* value maps generated using a two-tailed (nondirected) paired *t* test to identify voxels with activity differences between conditions (3dttest++). For between-group analysis (Fig. 4 and table S5), *t* value maps were generated using a two-tailed, two-sample *t* test between groups. The voxel-wise threshold was set to $P < 0.005$, and Monte Carlo simulation determined minimum cluster size and provided a cluster-wise corrected threshold of $P < 0.05$ within the whole-brain group mask. Notably, most reported effects were at more stringent significance levels than the threshold. We used a conservative nonparametric method simulating noise volumes by randomizing and permuting data (3dttest++ with the option "–Clustsim") (*46*).

Behavioral analysis

At each assessment, item recognition memory was assessed as the proportion of total trials that were correctly recognized as old (hits) or new (correct rejections). Similar results were obtained when considering only the high-confidence hit trials (for example, no effect of stimulation on item recognition accuracy; Post-Stim versus Post-Sham: $T_{15} = 0.57$, $P = 0.29$). Contextual recollection accuracy was assessed as the proportion of correct responses (one of six options), given that the object was correctly recognized with high confidence (certain response). The average of Pre-Stim and Pre-Sham assessment scores was used as Baseline. On the basis of a priori hypotheses of memory improvement due to stimulation, directional (one-tailed) paired (within-subjects) and two-sample (between-groups) *t* tests were used.

SUPPLEMENTARY MATERIALS

Supplementary material for this article is available at http://advances.sciencemag.org/cgi/content/full/4/8/eaar2768/DC1

Table S1. fMRI activity in individual regions of the PM network.
Table S2. fMRI activity in individual regions of the AT network.
Table S3. Clusters showing increased activity due to parietal stimulation (Post-Stim versus Post-Sham).
Table S4. Activity changes due to prefrontal active control stimulation.
Table S5. Clusters showing greater activity increases (Post-Stim versus Post-Sham) due to parietal stimulation versus control prefrontal stimulation.

REFERENCES AND NOTES

1. W. B. Scoville, B. Milner, Loss of recent memory after bilateral hippocampal lesions. *J. Neurol. Neurosurg. Psychiatry* **20**, 11–21 (1957).
2. F. P. Battaglia, K. Benchenane, A. Sirota, C. M. A. Pennartz, S. I. Wiener, The hippocampus: Hub of brain network communication for memory. *Trends Cogn. Sci.* **15**, 310–318 (2011).
3. R. L. Buckner, J. R. Andrews-Hanna, D. L. Schacter, The brain's default network: Anatomy, function, and relevance to disease. *Ann. N. Y. Acad. Sci.* **1124**, 1–38 (2008).
4. H. Eichenbaum, A cortical–hippocampal system for declarative memory. *Nat. Rev. Neurosci.* **1**, 41–50 (2000).
5. C. Ranganath, M. Ritchey, Two cortical systems for memory-guided behaviour. *Nat. Rev. Neurosci.* **13**, 713–726 (2012).
6. J. P. Aggleton, M. M. Albasser, D. J. Aggleton, G. L. Poirier, J. M. Pearce, Lesions of the rat perirhinal cortex spare the acquisition of a complex configural visual discrimination yet impair object recognition. *Behav. Neurosci.* **124**, 55–68 (2010).
7. M. C. Alvarado, J. Bachevalier, Comparison of the effects of damage to the perirhinal and parahippocampal cortex on transverse patterning and location memory in rhesus macaques. *J. Neurosci.* **25**, 1599–1609 (2005).
8. L. Davachi, J. P. Mitchell, A. D. Wagner, Multiple routes to memory: Distinct medial temporal lobe processes build item and source memories. *Proc. Natl. Acad. Sci. U.S.A.* **100**, 2157–2162 (2003).
9. G. Norman, M. J. Eacott, Dissociable effects of lesions to the perirhinal cortex and the postrhinal cortex on memory for context and objects in rats. *Behav. Neurosci.* **119**, 557–566 (2005).
10. B. P. Staresina, K. D. Duncan, L. Davachi, Perirhinal and parahippocampal cortices differentially contribute to later recollection of object- and scene-related event details. *J. Neurosci.* **31**, 8739–8747 (2011).
11. M. S. Fanselow, H.-W. Dong, Are the dorsal and ventral hippocampus functionally distinct structures? *Neuron* **65**, 7–19 (2010).
12. I. Kahn, J. R. Andrews-Hanna, J. L. Vincent, A. Z. Snyder, R. L. Buckner, Distinct cortical anatomy linked to subregions of the medial temporal lobe revealed by intrinsic functional connectivity. *J. Neurophysiol.* **100**, 129–139 (2008).
13. J. Poppenk, H. R. Evensmoen, M. Moscovitch, L. Nadel, Long-axis specialization of the human hippocampus. *Trends Cogn. Sci.* **17**, 230–240 (2013).
14. S. Qin, X. Duan, K. Supekar, H. Chen, T. Chen, V. Menon, Large-scale intrinsic functional network organization along the long axis of the human medial temporal lobe. *Brain Struct. Funct.* **221**, 3237–3258 (2016).
15. M. Ritchey, L. A. Libby, C. Ranganath, Cortico-hippocampal systems involved in memory and cognition: The PMAT framework. *Prog. Brain Res.* **219**, 45–64 (2015).
16. M. S. Copara, A. S. Hassan, C. T. Kyle, L. A. Libby, C. Ranganath, A. D. Ekstrom, Complementary roles of human hippocampal subregions during retrieval of spatiotemporal context. *J. Neurosci.* **34**, 6834–6842 (2014).
17. J. S. Damoiseaux, R. P. Viviano, P. Yuan, N. Raz, Differential effect of age on posterior and anterior hippocampal functional connectivity. *NeuroImage* **133**, 468–476 (2016).
18. M. Ritchey, A. P. Yonelinas, C. Ranganath, Functional connectivity relationships predict similarities in task activation and pattern information during associative memory encoding. *J. Cogn. Neurosci.* **26**, 1085–1099 (2014).
19. A. D. Boes, S. Prasad, H. Liu, Q. Liu, A. Pascual-Leone, V. S. Caviness Jr., M. D. Fox, Network localization of neurological symptoms from focal brain lesions. *Brain* **138**, 3061–3075 (2015).
20. R. N. Henson, A. Greve, E. Cooper, M. Gregori, J. S. Simons, L. Geerligs, S. Erzinçlioğlu, N. Kapur, G. Browne, The effects of hippocampal lesions on MRI measures of structural and functional connectivity. *Hippocampus* **26**, 1447–1463 (2016).
21. C. Gratton, E. M. Nomura, F. Pérez, M. D'Esposito, Focal brain lesions to critical locations cause widespread disruption of the modular organization of the brain. *J. Cogn. Neurosci.* **24**, 1275–1285 (2012).
22. D. E. Warren, N. L. Denburg, J. D. Power, J. Bruss, E. J. Waldron, H. Sun, S. E. Petersen, D. Tranel, Brain network theory can predict whether neuropsychological outcomes will differ from clinical expectations. *Arch. Clin. Neuropsychol.* **32**, 40–52 (2017).
23. J. X. Wang, L. M. Rogers, E. Z. Gross, A. J. Ryals, M. E. Dokucu, K. L. Brandstatt, M. S. Hermiller, J. L. Voss, Targeted enhancement of cortical-hippocampal brain networks and associative memory. *Science* **345**, 1054–1057 (2014).
24. A. S. Nilakantan, D. J. Bridge, E. P. Gagnon, S. A. VanHaerents, J. L. Voss, Stimulation of the posterior cortical-hippocampal network enhances precision of memory recollection. *Curr. Biol.* **27**, 465–470 (2017).
25. S. Canals, M. Beyerlein, H. Merkle, N. K. Logothetis, Functional MRI evidence for LTP-induced neural network reorganization. *Curr. Biol.* **19**, 398–403 (2009).

26. M.-M. Mesulam, G. W. Van Hoesen, D. N. Pandya, N. Geschwind, Limbic and sensory connections of the inferior parietal lobule (area PG) in the rhesus monkey: A study with a new method for horseradish peroxidase histochemistry. *Brain Res.* **136**, 393–414 (1977).
27. E. J. Mufson, D. N. Pandya, Some observations on the course and composition of the cingulum bundle in the rhesus monkey. *J. Comp. Neurol.* **225**, 31–43 (1984).
28. K. A. Paller, A. D. Wagner, Observing the transformation of experience into memory. *Trends Cogn. Sci.* **6**, 93–102 (2002).
29. L. A. Libby, A. D. Ekstrom, J. D. Ragland, C. Ranganath, Differential connectivity of perirhinal and parahippocampal cortices within human hippocampal subregions revealed by high-resolution functional imaging. *J. Neurosci.* **32**, 6550–6560 (2012).
30. M. E. Raichle, The brain's default mode network. *Annu. Rev. Neurosci.* **38**, 433–447 (2015).
31. H. Kim, Neural activity that predicts subsequent memory and forgetting: A meta-analysis of 74 fMRI studies. *NeuroImage* **54**, 2446–2461 (2011).
32. H. Eichenbaum, Prefrontal-hippocampal interactions in episodic memory. *Nat. Rev. Neurosci.* **18**, 547–558 (2017).
33. X.-W. Yu, M. M. Oh, J. F. Disterhoft, CREB, cellular excitability, and cognition: Implications for aging. *Behav. Brain Res.* **322**, 206–211 (2017).
34. T. P. Vogels, K. Rajan, L. F. Abbott, Neural network dynamics. *Annu. Rev. Neurosci.* **28**, 357–376 (2005).
35. E. Álvarez-Salvado, V. Pallarés, A. Moreno, S. Canals, Functional MRI of long-term potentiation: Imaging network plasticity. *Philos. Trans. R. Soc. Lond. B Biol. Sci.* **369**, 20130152 (2013).
36. H. Eichenbaum, A. R. Yonelinas, C. Ranganath, The medial temporal lobe and recognition memory. *Annu. Rev. Neurosci.* **30**, 123–152 (2007).
37. R. La Joie, B. Landeau, A. Perrotin, A. Bejanin, S. Egret, A. Pélerin, F. Mézenge, S. Belliard, V. De La Sayette, F. Eustache, B. Desgranges, G. Chételat, Intrinsic connectivity identifies the hippocampus as a main crossroad between Alzheimer's and semantic dementia-targeted networks. *Neuron* **81**, 1417–1428 (2014).
38. M. M. Mesulam, Large-scale neurocognitive networks and distributed processing for attention, language, and memory. *Ann. Neurol.* **28**, 597–613 (1990).
39. S. Rossi, M. Hallett, P. M. Rossini, A. Pascual-Leone; Safety of TMS Consensus Group, Safety, ethical considerations, and application guidelines for the use of transcranial magnetic stimulation in clinical practice and research. *Clin. Neurophysiol.* **120**, 2008–2039 (2009).
40. D. A. Feinberg, T. G. Reese, V. J. Wedeen, Simultaneous echo refocusing in EPI. *Magn. Reson. Med.* **48**, 1–5 (2002).
41. A. Thielscher, A. Antunes, G. B. Saturnino, Field modeling for transcranial magnetic stimulation: A useful tool to understand the physiological effects of TMS? *Conf. Proc. IEEE Eng. Med. Biol. Soc.* **2015**, 222–225 (2015).
42. T. F. Brady, T. Konkle, G. A. Alvarez, A. Oliva, Visual long-term memory has a massive storage capacity for object details. *Proc. Natl. Acad. Sci. U.S.A.* **105**, 14325–14329 (2008).
43. D. E. Hannula, D. Tranel, N. J. Cohen, The long and the short of it: Relational memory impairments in amnesia, even at short lags. *J. Neurosci.* **26**, 8352–8359 (2006).
44. R. W. Cox, AFNI: Software for analysis and visualization of functional magnetic resonance neuroimages. *Comput. Biomed. Res.* **29**, 162–173 (1996).
45. M. Xia, J. Wang, Y. He, BrainNet Viewer: A network visualization tool for human brain connectomics. *PLOS ONE* **8**, e68910 (2013).
46. R. W. Cox, G. Chen, D. R. Glen, R. C. Reynolds, P. A. Taylor, FMRI clustering in AFNI: False-positive rates redux. *Brain Connect.* **7**, 152–171 (2017).

Acknowledgments: We thank M. M. Gunlogson, J. O'Neil, and E. P. Gagnon for the assistance with data collection; L. Libby and M. Ritchey for the details regarding regions of interest for fMRI analyses; and J. Disterhoft and C. Weiss for the helpful discussion. Neuroimaging was performed at the Northwestern University Center for Translational Imaging, supported by the Northwestern University Department of Radiology. **Funding:** This research was supported, in part, through the computational resources and staff contributions provided for Quest, the high-performance computing facility at Northwestern University, which is jointly supported by the Office of the Provost, the Office for Research, and Northwestern University Information Technology. This research was supported by R01-MH106512 from the National Institute of Mental Health, T32-AG20506 and F31-AG057109 from the National Institute on Aging, and T32-NS047987 from the National Institute of Neurological Disorders and Stroke. The content is solely the responsibility of the authors and does not necessarily represent the official view of the NIH. **Author contributions:** S.K., M.S.H., and J.L.V. designed the study. A.S.N., M.S.H., and R.T.P. collected the data. S.K., A.S.N., M.S.H., and J.L.V. performed the analyses. S.V. supervised participant eligibility and safety. All authors discussed the findings and wrote the manuscript. **Competing interests:** The authors declare that they have no competing interests. **Data and materials availability:** All data needed to evaluate the conclusions in the paper are present in the paper and/or the Supplementary Materials. All raw MRI data are archived in a public repository available with registration at http://nunda.northwestern.edu. Additional data related to this paper may be requested from the authors.

Submitted 20 October 2017
Accepted 18 July 2018
Published 22 August 2018
10.1126/sciadv.aar2768

Citation: S. Kim, A. S. Nilakantan, M. S. Hermiller, R. T. Palumbo, S. VanHaerents, J. L. Voss, Selective and coherent activity increases due to stimulation indicate functional distinctions between episodic memory networks. *Sci. Adv.* **4**, eaar2768 (2018).

ScienceAdvances

Selective and coherent activity increases due to stimulation indicate functional distinctions between episodic memory networks

Sungshin Kim, Aneesha S. Nilakantan, Molly S. Hermiller, Robert T. Palumbo, Stephen VanHaerents and Joel L. Voss

Sci Adv **4** (8), eaar2768.
DOI: 10.1126/sciadv.aar2768